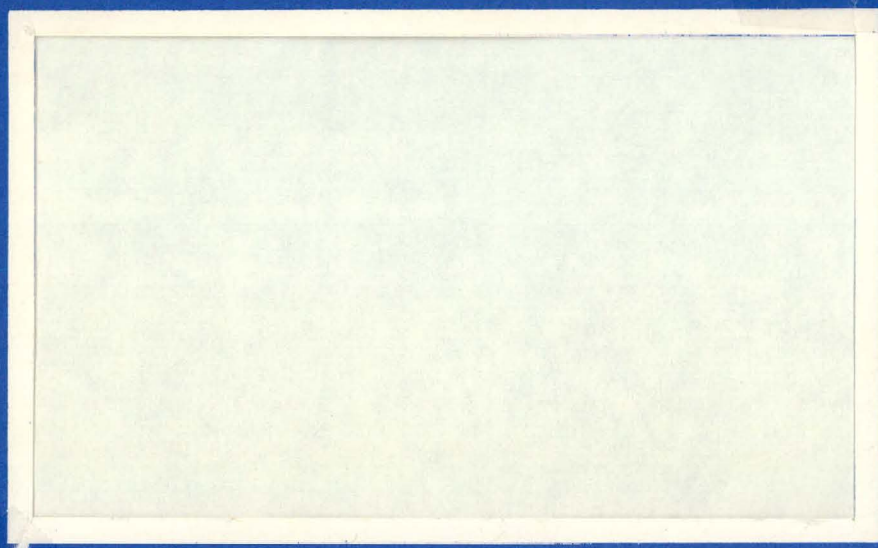


226
10-20 C

DWR-1595



MASTER



THIS DOCUMENT CONFIRMED AS
UNCLASSIFIED
DIVISION OF CLASSIFICATION
BY J.H. Kuhn / amh
DATE 10/22/70



WADCO
CORPORATION

a subsidiary of Westinghouse Electric Corporation
Post Office Box 1970
Richland, Washington 99352



DISTRIBUTION OF THIS DOCUMENT IS UNLIMITED

P7116

DISCLAIMER

This report was prepared as an account of work sponsored by an agency of the United States Government. Neither the United States Government nor any agency Thereof, nor any of their employees, makes any warranty, express or implied, or assumes any legal liability or responsibility for the accuracy, completeness, or usefulness of any information, apparatus, product, or process disclosed, or represents that its use would not infringe privately owned rights. Reference herein to any specific commercial product, process, or service by trade name, trademark, manufacturer, or otherwise does not necessarily constitute or imply its endorsement, recommendation, or favoring by the United States Government or any agency thereof. The views and opinions of authors expressed herein do not necessarily state or reflect those of the United States Government or any agency thereof.

DISCLAIMER

Portions of this document may be illegible in electronic image products. Images are produced from the best available original document.



LEGAL NOTICE

This report was prepared as an account of work sponsored by the United States Government. Neither the United States nor the United States Atomic Energy Commission, nor any of their employees, nor any of their contractors, subcontractors, or their employees, makes any warranty, express or implied, or assumes any legal liability or responsibility for the accuracy, completeness or usefulness of any information, apparatus, product or process disclosed, or represents that its use would not infringe privately owned rights.

HANFORD ENGINEERING DEVELOPMENT LABORATORY

Richland, Washington
operated by

WADCO CORPORATION

A Subsidiary of Westinghouse Electric Corporation
for the

United States Atomic Energy Commission Under Contract No. AT(45-1)-2170



UNIAXIAL AND BIAXIAL CREEP-RUPTURE
OF TYPE 316 STAINLESS STEEL
AFTER FAST REACTOR IRRADIATION^(a)

A. J. Lovell

R. W. Barker

LEGAL NOTICE

This report was prepared as an account of work sponsored by the United States Government. Neither the United States nor the United States Atomic Energy Commission, nor any of their employees, nor any of their contractors, subcontractors, or their employees, makes any warranty, express or implied, or assumes any legal liability or responsibility for the accuracy, completeness or usefulness of any information, apparatus, product or process disclosed, or represents that its use would not infringe privately owned rights.

September 1970

FIRST UNRESTRICTED
DISTRIBUTION MADE

OCT 2 '70



WADCO
CORPORATION

Richland, Washington 99352

- (a) Work performed by Battelle Northwest under Contract No. AT(45-1)-1830. Presented as BNWL-SA-3295 at the ASTM Symposium on Effects of Radiation on Structural Materials, June 29-July 2, 1970, at Niagara Falls, Canada

UNCLASSIFIED

DISTRIBUTION OF THIS DOCUMENT IS UNLIMITED

Printed in the United States of America
Available from
Clearinghouse for Federal Scientific and Technical Information
National Bureau of Standards, U.S. Department of Commerce
Springfield, Virginia 22151
Price: Printed Copy \$3.00; Microfiche \$0.65

UNIAXIAL AND BIAXIAL CREEP-RUPTURE
OF TYPE 316 STAINLESS STEEL
AFTER FAST REACTOR IRRADIATION

A. J. Lovell and R. W. Barker

ABSTRACT

The degradation in creep-rupture properties of Type 316 stainless steel after fast reactor irradiation has been determined for both uniaxial and biaxial loading conditions. Uniaxial specimens (rod-type) and biaxial specimens (tube-type) were irradiated in the 7C4 position of the EBR-II to a total fluence of 1.2×10^{22} n/cm² [1×10^{22} n/cm² ($E > 0.1$ MeV)] at ~ 480 °C. Postirradiation tests were performed over the temperature range 538 to 760 °C.

The results from both uniaxial and biaxial tests at 538 °C show significant losses in rupture life relative to unirradiated specimens when compared on the basis of initial true stress. Rupture life was reduced by factors down to 1/20 for uniaxial and by factors down to 1/40 for biaxial tests. The substantial loss in rupture life at 538 °C was primarily a result of high creep rates, and the contribution from ductility loss was relatively small. Uniaxial test results at 593 °C show reductions in rupture life of a factor of 1/5 at high stresses and only small reductions at low stresses. The rupture life for both uniaxial and biaxial tests at 649 °C show only a factor of 1/2 decrease after irradiation. The decrease becomes more substantial again at 760 °C with a factor of 1/10 to 1/7 reduction in life. The rupture life reductions at 593, 649, and 760 °C were the results of reduced ductility, with no significant contributions from creep rate differences. The underlying cause of the low ductility at these higher temperatures is associated with helium embrittlement and defect structure.

Key Words: *Creep, stress-rupture, irradiation, structural materials, fast reactor, creep rate, austenitic stainless steel, AISI Type 316, rupture life, ductility.*

**THIS PAGE
WAS INTENTIONALLY
LEFT BLANK**

TABLE OF CONTENTS

ABSTRACT	iii
LIST OF FIGURES	vi
INTRODUCTION	1
SUMMARY	1
EXPERIMENTAL PROCEDURE	2
Materials	2
Irradiation	4
Test Methods	5
RESULTS	8
Rupture Life	8
Temperature-Compensated Rupture Life	13
Creep Rates	13
Ductility	17
DISCUSSION	17
REFERENCES	23

LIST OF FIGURES

1	Hoop Stress-Strain Curve for 5.3 mm Diameter x 0.2 mm Wall Type 316 SS Subjected to Internal Pressure	7
2	Effect of EBR-II Irradiation on the Rupture Life of Type 316 SS Determined in Uniaxial Tests	10
3	Effect of EBR-II Irradiation on the Rupture Life of Type 316 SS Determined in Biaxial Tests	14
4	Effect of EBR-II Irradiation on the Theta Correlation of Uniaxial Test Results on Type 316 SS	15
5	Effect of EBR-II Irradiation on the Theta Correlation of Biaxial Test Results on Type 316 SS	16
6	Effect of EBR-II Irradiation on the Minimum Rate of Type 316 SS determined in Uniaxial Tests	18
7	Effect of EBR-II Irradiation on Average Creep Rate of Type 316 SS Tube Determined in Biaxial Tests	18

UNIAXIAL AND BIAXIAL CREEP-RUPTURE
OF TYPE 316 STAINLESS STEEL
AFTER FAST REACTOR IRRADIATION

A. J. Lovell and R. W. Barker

INTRODUCTION

The selection of AISI 316 stainless steel (SS) as a prime alloy for application in liquid metal fast breeder reactor systems has prompted a need to know how this alloy is affected by fast neutron irradiation at elevated temperatures. Only limited data on the postirradiation mechanical properties obtained from fast reactor experiments are available for this alloy. This limitation is particularly acute for the time dependent creep and creep-rupture properties. To obtain such information, creep tests have been made on Type 316 SS after fast reactor irradiation in the Experimental Breeder Reactor-II (EBR-II). These tests were designed to determine empirically the stress dependence of minimum creep rate and rupture life and the ductility of this irradiated alloy over the temperature range 538 to 760 °C. Both a uniaxial loading condition on conventional tensile specimens and a biaxial loading condition on pressurized tube specimens were included in this investigation. This study shows that creep and creep-rupture properties were changed significantly as a result of irradiation, and discusses possible explanations for the observed property changes.

SUMMARY

Fast reactor irradiation to a total fluence of 1×10^{22} n/cm² at a temperature of 482 °C resulted in a significant degradation of the creep-rupture properties of Type 316 SS. High creep rates, possibly resulting from irradiation-induced precipitation, led to a substantial loss in rupture life at a

test temperature of 538 °C. Low ductility, probably attributable to helium embrittlement, was responsible for reduced rupture life in the temperature range 593 to 760 °C.

Results from both uniaxial tests and biaxial tests showed similar changes in rupture life when comparisons were based on initial true stress. Because of substantial differences in initial plastic strain between unirradiated and irradiated specimens, changes in rupture life measure in high-stress biaxial tests were substantially smaller when the comparison was made on the basis of engineering stress.

EXPERIMENTAL PROCEDURE

MATERIALS

The chemical composition of the two Type 316 SS used for the uniaxial and biaxial specimens are shown in Table 1. The only significant differences in chemical composition between the two materials were in the carbon and manganese contents.

The material for uniaxial specimens was received as a 15.9 mm rod; this rod was reduced to a diameter of 7.75 mm by cold swaging with intermediate anneals at 1065 °C. In the final cold-swaging, the diameter was reduced from 7.75 to 6.86 mm. The rod was given a final anneal at 1065 °C for one hour, followed by a rapid air cool. The grain size of this material was ASTM 5 to 6. Tensile specimens with a gage section diameter of 3.18 mm and a gage section length of 26.5 mm were then machined from the rod.

The test material for biaxial specimens was 5.3 mm diameter by 0.2 mm wall Type 316 SS tubing in the as-received condition. The as-received condition contains a small amount of cold work, which is shown by the following room temperature yield strength values for as-received and annealed (1065 °C, one hour) tube specimens:

TABLE 1. Chemical Composition of Type 316 SS
Used in Uniaxial and Biaxial Creep-
Rupture Studies

<u>Element</u>	<u>Composition, wt%</u>		
	<u>Specimen Type</u>		
	<u>Uniaxial</u>		<u>Biaxial</u>
	<u>(a)</u>	<u>(b)</u>	
C	0.057	0.052	0.081
Mn	1.80	1.72	1.51
P	0.024	0.012	
S	0.014	0.020	
Si	0.36	0.38	0.50
Ni	13.39	13.55	13.25
Cr	17.71	17.80	17.84
Mo	2.26	2.33	2.32
Cu	0.18	0.20	0.05
Co	0.13	0.14	
N ₂		0.041	0.039
V		0.04	
Ti		0.003	
Al		0.026	
B		<0.005	
O ₂		0.0178	

a. Vendor Analysis

b. Independent Analysis

<u>Material Condition</u>	<u>0.2% Offset Yield Strength, psi</u>
As-received	38,000
	39,000
Annealed	33,400
	33,800

The grain size of the as-received material is about ASTM 7-8. Biaxial stress-rupture specimens were composed of a section of the tubing to which appropriate fittings have been attached. This resulted in a test specimen having a length-to-diameter ratio of about 6.

IRRADIATION

The uniaxial and biaxial test specimens were sealed in Type 316 SS capsules in an environment of pure sodium containing 12 to 15 ppm O_2 , 29 ppm C, 25 ppm Si, 110 ppm K, and 10 ppm Ca. Boron, magnesium, manganese, and others were identified as being present in trace quantities. These capsules were placed in Mk B-7 type tubes normally used for structural materials irradiation in EBR-II. An annular gas gap filled with a 30% He-70% Ar mixture was used in conjunction with nuclear heating to achieve an irradiation temperature estimated to be ~ 482 °C. This estimate was based on heat transfer calculations using best available information on reactor sodium temperature for the assembly, experiment geometry, and reactor gamma heat (~ 0.84 W/g). However, the observed microstructure and the postirradiation tensile properties for the rod specimens, when compared with other irradiated materials, indicated the irradiation temperature had been 540 °C or higher. Irradiations were conducted in position 7C4 of EBR-II within the core region. Both sets of specimens were irradiated to a fluence of $1.2 \times 10^{22} \pm 15\%$ (total) [1.0×10^{22} n/cm² (E > 0.1 MeV)]. The irradiation period was equivalent to 127 full

power days (3045 hours). After irradiation, the sodium environment was removed by dissolving and rinsing with water followed by rinsing with ethyl alcohol for drying purposes.

TEST METHODS

The basic standard for test procedure was the ASTM tentative recommended practice for conducting creep and time-to-rupture tension tests of materials, ASTM E139-66T (revised 1966). Uniaxial and biaxial stress tests were conducted within the recommended ASTM specifications for temperature and stress. Uniaxial tests were conducted within the ASTM recommendations for alignment.

All uniaxial tests were conducted in an inert gas (helium or argon) environment. The test procedure allowed 20 hours for heatup and thermal stabilization prior to applying the creep load. Specimen extension was monitored during the test by measuring pull-rod motion with a dial indicator. Total elongations were obtained in two ways. One value was obtained by post-test measurement of specimen length and a second value was estimated from the strain-time curves.

Biaxial stress-rupture tests were conducted in an argon atmosphere by internally pressurizing unrestrained thin-wall tubes with argon gas and holding pressure constant until rupture occurred. Under these conditions, the initial hoop stress to axial stress ratio is 2. Maximum engineering hoop stress was determined using the formula for thin wall cylinders:

$$\sigma = \frac{PD}{2t}$$

where P = internal gas pressure

D = original inside diameter of tube

t = original minimum wall thickness of tube.

Tests were conducted by attaching the tubular cladding specimen to a test rig through the use of standard tube fittings,

placing the assembled specimen-test rig in a heated furnace, and applying the desired pressure after the specimen had stabilized (~4 hours) at the desired test temperature.

Diametral strain for biaxial stress-rupture tests were not measured at the point of maximum strain on fragmented test pieces to avoid confusing uniform strain with strain which is related to sudden gas expulsion at the time of failure. It was empirically determined that a diameter measurement taken halfway between the ruptured area and the end fitting, using the longest part of the fragmented specimen, gave a reasonably good value of uniform strain.

The uniaxial and biaxial tests were conducted at constant load and pressure, respectively. At particular test temperatures and stresses, substantial plastic straining occurred during initial application of load (pressure). The increased flow stress of irradiated material reduced the initial strain on loading with respect to the strain obtained on loading an unirradiated specimen. This difference in initial strain resulted in a lower true stress in irradiated specimens than in unirradiated specimens with identical loads (pressure). All comparisons were therefore based on true initial stress.

True initial stress values for uniaxial tests were calculated as $\sigma_0(1 + \epsilon_L)$, where σ_0 is the engineering creep stress and ϵ_L is the engineering strain in a fully loaded creep specimen. Values of ϵ_L were determined from tensile tests at each temperature on both irradiated and unirradiated specimens.

The relationship of strain in the biaxially loaded specimen to the internal gas pressure during loading was determined by subjecting a specimen to an ascending series of test pressures, holding for one minute period, and measuring the strain produced. A stress-strain curve was constructed, as shown in Figure 1.

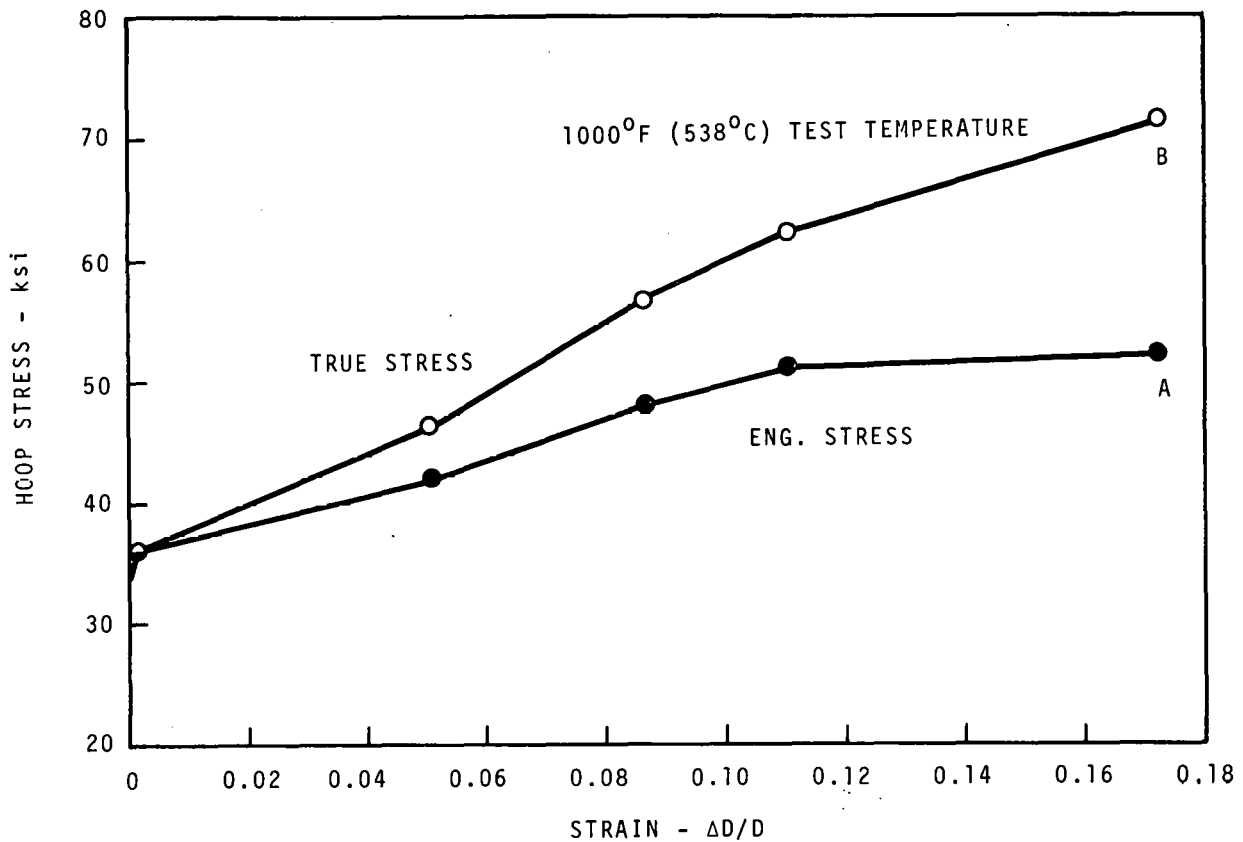


FIGURE 1. Hoop Stress-Strain Curve for 5.3 mm Diameter x 0.2 mm Wall Type 316 SS Subjected to Internal Pressure

Curve A is the engineering stress, σ_o , based on original dimensions, and Curve B is the true stress, calculated as $\sigma_o(1 + \epsilon)^2$, where ϵ is the engineering diametral strain. In each test, the instantaneous strain is obtained from Line A and the true stress is obtained from Line B for that strain.

Attempts to establish Curves A and B at 538 °C on irradiated tubes which show low initial strain indicated there was very little difference in the true and engineering hoop stress; thus engineering initial hoop stress was used for all biaxial tests on irradiated tubes.

The average creep rate of biaxial test specimens was evaluated by separating the strain caused by creep and the strains associated with initial load-up and with the geometric changes

during creep. The creep component of the total strain was obtained by first determining the final true hoop stress, $\sigma_o(1 + \epsilon_r)^2$, from the rupture strain, ϵ_r , and using this stress in conjunction with Line B of Figure 1 to determine the tensile strain, ϵ_t . Then ϵ_t was subtracted from ϵ_r to obtain ϵ_c , the creep strain. For the low strain obtained in the irradiated tubes, ϵ_c was assumed to be equal to ϵ_r . Average creep rate values were then calculated by dividing the creep strain, ϵ_c , by the rupture time.

RESULTS

RUPTURE LIFE

The uniaxial creep and creep-rupture results for tests determined at 538, 593, 649, and 760 °C are given in Table 2. The stress dependence of rupture life is shown on a conventional log stress-log rupture time plot in Figure 2. In general, the curve plotted for the irradiated specimens is parallel, or nearly parallel, to the curve for unirradiated specimens, except at 593 °C where the rupture life of irradiated specimens exhibits a somewhat higher stress dependence than does the rupture life of unirradiated specimens. The rupture life of all irradiated specimens was reduced when compared to unirradiated control material. The reduction in rupture life at 538 °C was about a factor of 1/20. Losses in rupture life at 593 and 649 °C were less severe, with reductions by factors of 1/5 to 1/2 and 1/2, respectively. At 760 °C, the reduction in rupture life was about a factor of 1/7.

Biaxial stress-rupture results on the as-received material determined at 538, 649, and 760 °C are given in Table 3. These results are in reasonable agreement with stress-rupture data published by other experimenters.^(1,2) The results determined at the same temperatures for irradiated material are given in Table 4.

TABLE 2. Uniaxial Creep-Rupture Data for Type 316 SS Irradiated in EBR-II (a)
to 1.2×10^{22} n/cm² (total) at ~ 900 °F (482 °C)

Test Temp, °C	Eng. Stress, ksi	True Init. Stress, ksi		Minimum Creep Rate $\times 10^5$, in./in./hr		Rupture Time, hr		Total % Elongation	
		Irrad.	Control	Irrad.	Control	Irrad.	Control	Irrad.	Control
538	55	60.2	64.2	107.0	9.3	26.7	263	17.6	38.9
538	50	53.0	56.5	31.9	3.3	85.2	433	12.3	18.2
538	45	47.1	49.5	24.2	1.4/2.7	107.8	1032	5.8	15.4
538	40	41.1	43.1	6.3	0.8	149.6	2795	3.7	14
538	36	36.7	38.1	1.0	~ 0.27	> 673.5			
538	30	30.5	30.6	~ 0.1	~ 0.06	On Test			
593	45	46.8	50.0	489.0	250.0	11.5	23	14.1	~ 25.1
593	40	40.6	43.3	68.6	4.4/34.2	45.5	~ 200	7.9	25
593	36	36.6	38.4	23.2	~ 26.7	202.8	236	8.0	20.9
593	30	30.2	31.2	4.7	~ 5.2	> 1489			
593	26	26.1	26.7	0.9	~ 1.5	On Test			
649	30	30.3	31.1	~ 84.5	212.0	56.8	95		~ 50
649	28	28.1	28.8	~ 42.8	94.4	~ 130	168	~ 13	51
649	25	25.1	25.5	~ 25.0	63.8	262	375		66
649	22	22.1	22.2	10.1	15.9	~ 800	1295	~ 19	35
760	17	17	17.1	948	878	9.3	28	~ 8.8	72
760	15	15	15	~ 222.0	460/412	20.1	72	7.2	70
760	12	12	12	66	90.4	55.1	246	~ 4.5	64
760	10	10	10	23.2	28.5	146.5	1050	5.3	59

- a. All tests in inert gas
b. Estimated from creep curve
c. Test stopped before rupture
d. Extrapolated value

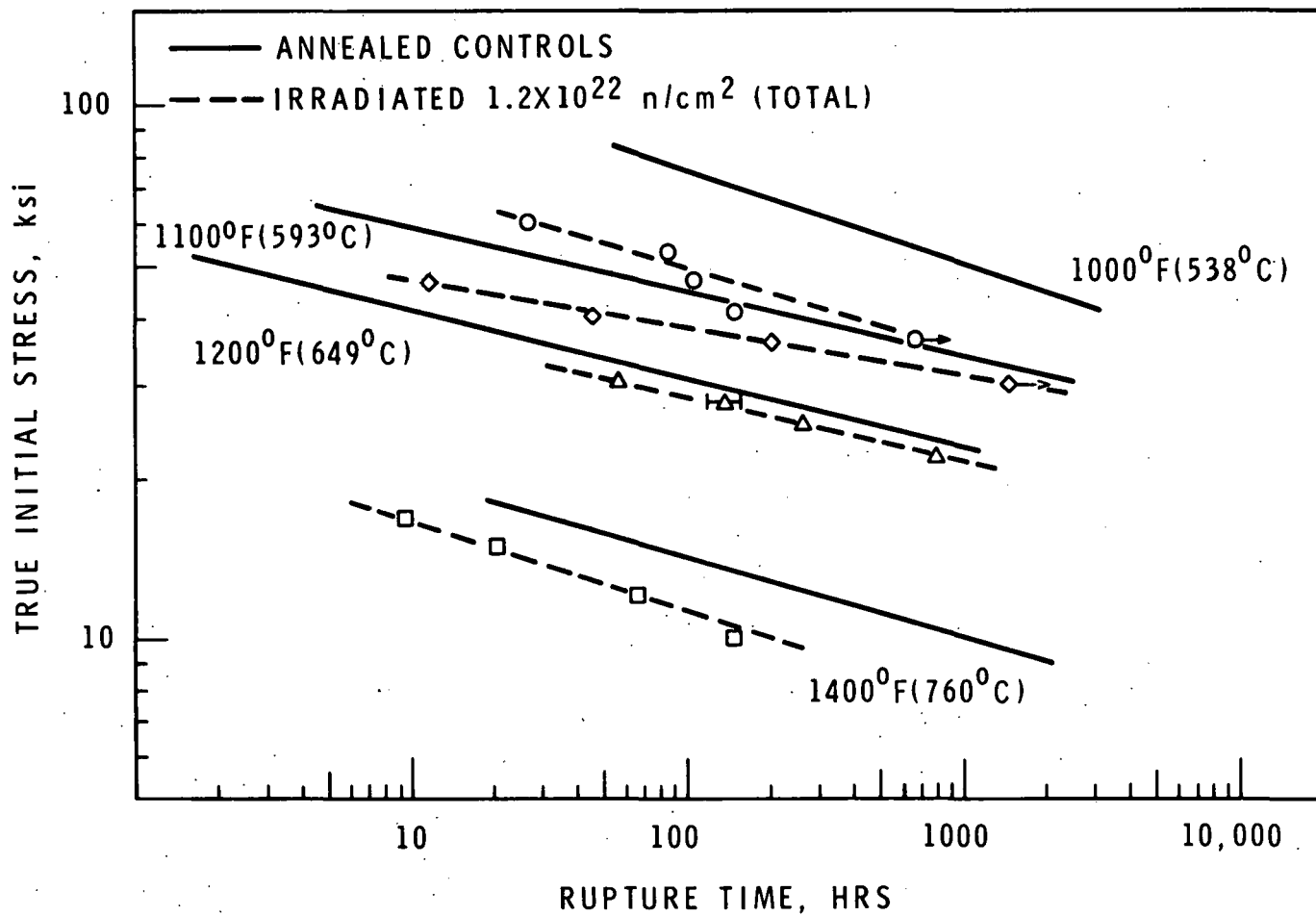


FIGURE 2. Effect of EBR-II Irradiation on the Rupture Life of Type 316 SS Determined in Uniaxial Tests

TABLE 3. Biaxial Stress-Rupture Data for Type 316 SS

Test Temp, °C	Hoop Stress, ksi		Rupture Time, hr	Ductility, $\Delta D/D$, %	Average Creep Rate $\times 10^5$, in./in./hr
	Eng.	Tr. Init.			
538	52.0	71.0	0.1	N.A.	N.A.
538	51.0	62.0	6.0	17.0	117.0
538	49.0	58.7	79.0	21.0	46.8
538	48.0	56.7	55.0	14.0	54.6
538	42.0	46.7	545.0	13.0	10.1
538	38.0	44.8	1681.0	8.7	2.56
649	38.5	44.0	0.5	16.5	1120.0
649	31.5	33.0	5.8	6.2	450.0
649	30.0	31.4	12.0	5.8	225.0
649	29.0	30.0	15.0	8.6	370.0
649	25.5	26.0	70.0	4.8	46.0
649	23.5	24.0	875.0	13.0	127.0
649	20.0	20.0	385.0	1.9	3.6
649	18.0	18.0	3470.0	6.7	1.93
649	17.0	17.0	1230.0	14.3	115.0
760	26.0	27.0	0.4	24.0	4350.0
760	19.8	20.0	6.8	19.2	2000.0
760	18.0	18.0	10.0	15.0	1400.0
760	17.0	17.0	16.0	13.9	800.0
760	13.9	13.9	42.0	21.5	512.0
760	9.6	9.6	300.0	9.1	31.0
760	6.5	6.5	1981.0	9.6	4.8

**TABLE 4. Biaxial Stress-Rupture Data for Type 316 SS
Irradiated in EBR-II to 1.2×10^{22} n/cm² (total)
at 900 °F (482 °C)**

Test Temp, °C	Eng. Hoop Stress, ksi ^(a)	Rupture Time, hr	Ductility, ΔD/D, %	Average Creep Rate x 10 ⁵ , in./in./hr
538	58.3	0.1	3.3	--
538	54.0	2.2	N.A.	N.A.
538	50.0	4.1	4.3	1000.0
538	50.0	9.6	3.8	397.0
538	49.0	29.0	N.A.	N.A.
538	46.0	22.0	2.9	132.0
538	40.0	140.0	1.0	10.0
649	36.0	0.6	9.7	9744.0
649	36.0	2.1	1.9	905.0
649	30.0	32.0	2.4	75.0
649	25.2	20.0	0.5	25.0
649	23.5	70.0	1.9	27.0
649	18.0	739.0	5.7	7.7
649	16.0	820.0	0.9	1.0
760	23.5	0.3	N.A.	N.A.
760	17.5	1.4	N.A.	N.A.
760	12.0	8.2	5.3	646.0
760	7.8	330.0	5.3	16.0

a. Engineering and true stress assumed to be the same for irradiated tubes

The biaxial stress-rupture data is plotted as log stress against log rupture time, in Figure 3. It was found that the irradiation reduced the rupture life of the Type 316 SS, when tested under biaxial stress conditions, at each of the test temperatures. At 538 °C, the reduction in rupture life is about a factor of 1/40. The decrease in rupture life at 649 °C was only a factor of 1/2, while at 760 °C, the reduction in rupture life was about a factor of 1/10.

TEMPERATURE-COMPENSATED RUPTURE LIFE

The uniaxial data and the biaxial data are presented in Figures 4 and 5 on log stress-log θ plots, where θ is defined as

$$\theta = t_r \exp \left(-\frac{Q}{RT} \right)$$

where t_r is rupture life in hours

Q is activation energy in calories/mole

T is absolute temperature in °K

R is gas constant in calories/mole-degree.

Results from preirradiation and postirradiation tests correlate well with a Q value of 95,000 calories/mole in both the uniaxial and biaxial tests. Since only two of the 538 °C uniaxial tests (at engineering stresses of 45 and 40 ksi) on irradiated specimens fall short of the curve; even within the 538 °C test series, it appears that these specimens failed prematurely. The temperature-compensated rupture life plots in Figures 4 and 5 clearly show the large reduction in rupture life at 538 °C, the lesser reductions at 593 and 649 °C, and the larger losses again at 760 °C.

CREEP RATES

The minimum creep rates determined in uniaxial tests on both irradiated and unirradiated material are given in Table 2. The results are plotted as log creep rate against log stress

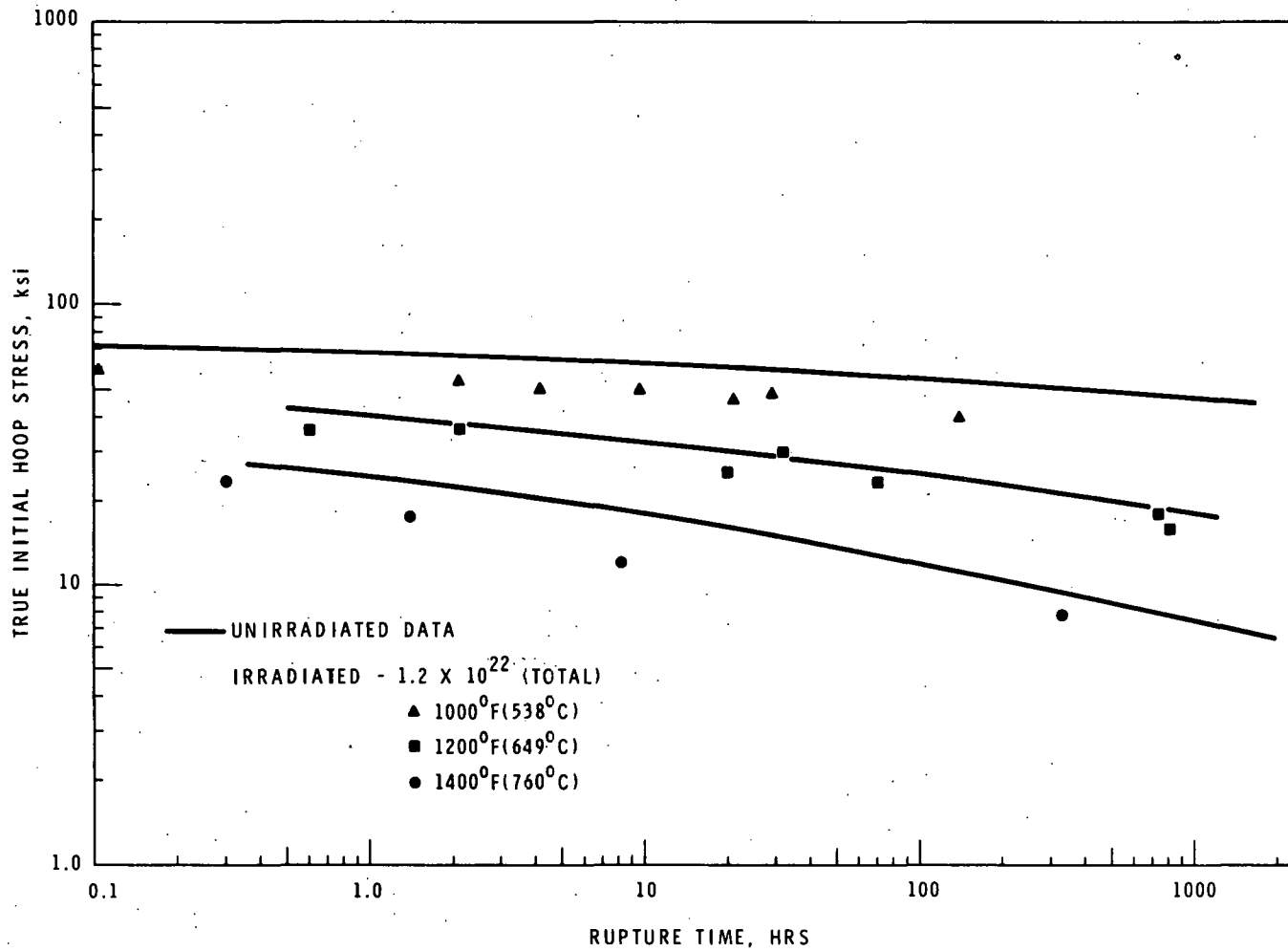


FIGURE 3. Effect of EBR-II Irradiation on the Rupture Life of Type 316 SS Determined in Biaxial Tests

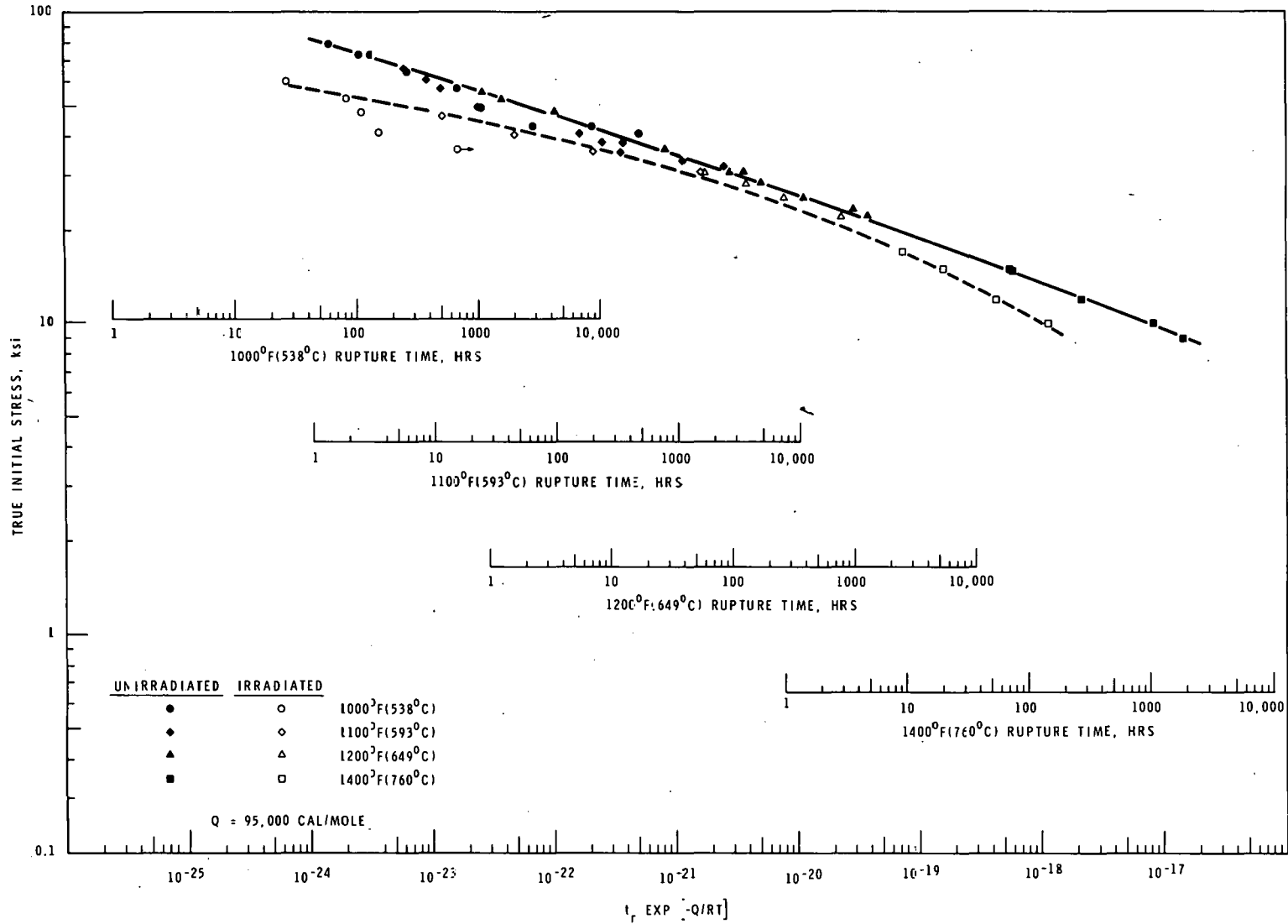


FIGURE 4. Effect of EBR-II Irradiation on the Theta Correlation of Uniaxial Test Results on Type 316 SS

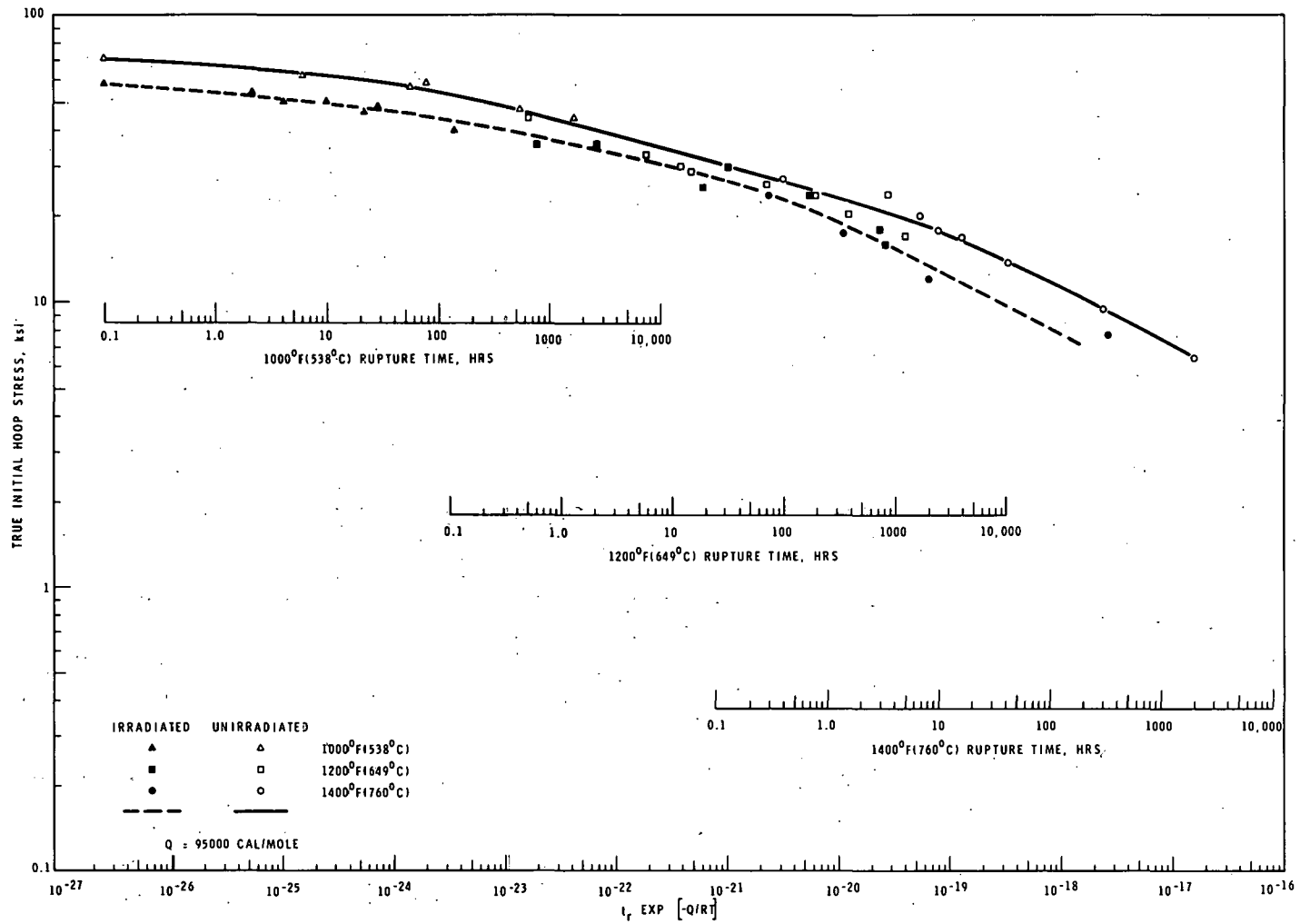


FIGURE 5. Effect of EBR-II Irradiation on the Theta Correlation of Biaxial Test Results on Type 316 SS

in Figure 6. The creep rate was found to increase significantly (i.e., by up to factor of 10) after irradiation for tests at 538 °C. The stress dependence of minimum creep rate appeared to be higher for irradiated material at this temperature. The magnitude and stress dependence of minimum creep rate do not appear to be changed significantly at test temperatures of 593, 649, and 760 °C.

Average creep rates determined from biaxial tests are presented graphically in Figure 7. These results also showed higher creep rates in irradiated material at a test temperature of 538 °C. The creep rates of irradiated specimens at 649 °C were virtually the same as the unirradiated values. Although the data at 760 °C is quite limited, it appeared that irradiated creep rate values were again higher than unirradiated values.

DUCTILITY

Strain at rupture in both uniaxial tests (see Table 2) and biaxial tests (see Tables 3 and 4) was reduced by irradiation. The lowest strains observed were about 5% for uniaxial tests and about 1% for biaxial tests. Comparison of the uniaxial strain-time curves revealed that both second stage creep strain and third stage creep strain are reduced in irradiated material at temperatures of 593 °C and above. Although the creep strains may be somewhat lower in irradiated material tested at 538 °C, the major factor affecting ductility at this temperature was reduced plastic strain on loading.

DISCUSSION

The results of this investigation show that fast reactor irradiation produces nearly the same changes in rupture life in uniaxial tests and in biaxial tests. This agreement between the two sets of test results shows that the basic material behavior is similar in both types of tests. However, it is important to emphasize that this conclusion is based on the

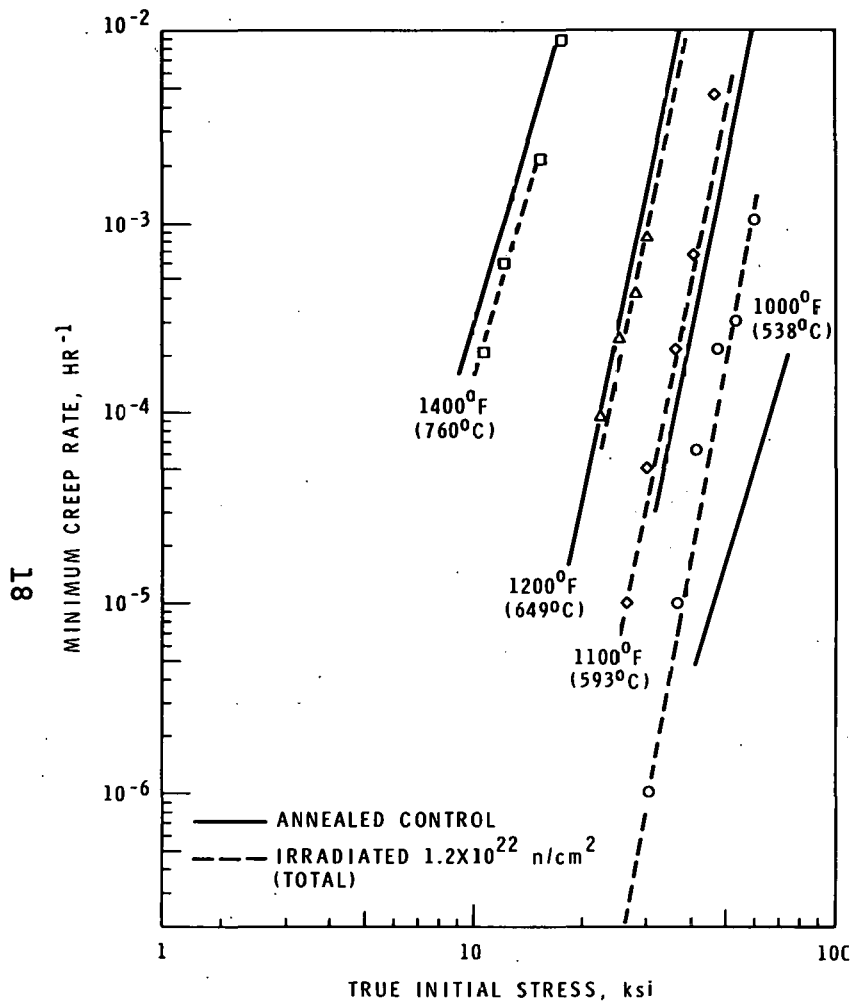


FIGURE 6. Effect of EBR-II Irradiation on the Minimum Creep Rate of Type 316 SS Determined in Uniaxial Tests

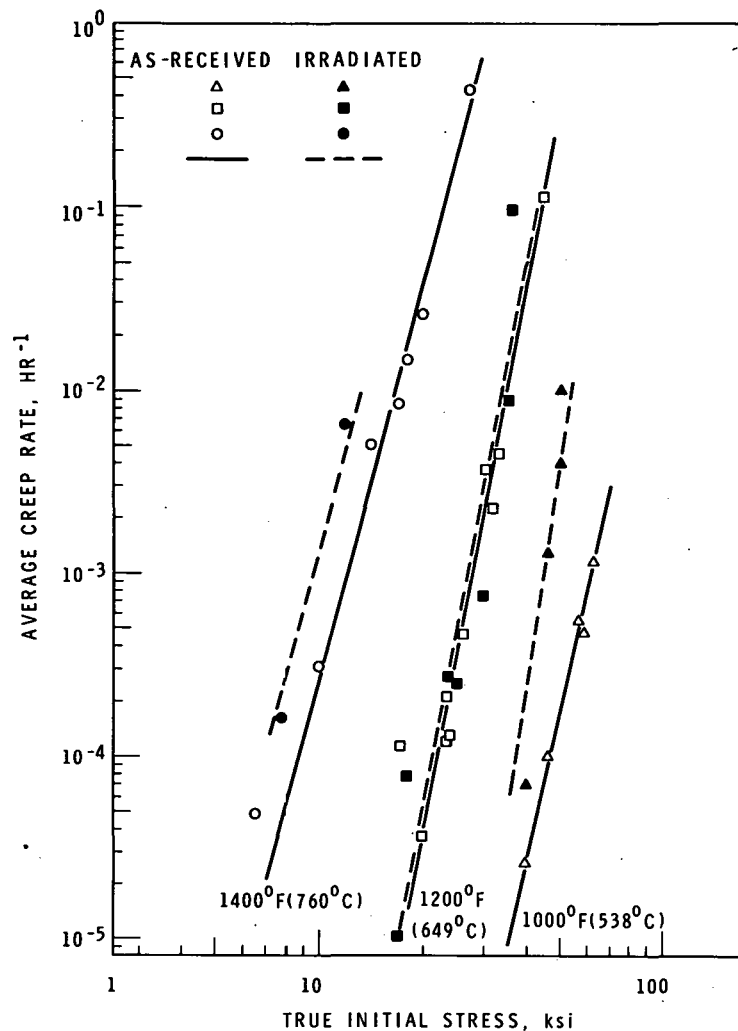


FIGURE 7. Effect of EBR-II Irradiation on Average Creep Rate of Type 316 SS Tube Determined in Biaxial Tests

the use of initial true stress in comparing results from unirradiated specimens with results from irradiated specimens. If comparisons are based on engineering stress, then uniaxial tests and biaxial tests do not show the same losses in rupture life at high stresses. For example, it was found that the reduction in rupture life at 538 °C, based on initial true stress, was about a factor of 1/40 in biaxial tests. If results for tests are compared on the basis of engineering stress, it is found that there is essentially no difference in rupture life at 538 °C. On the other hand, the reduction in rupture life in 538 °C uniaxial tests changes from a factor of 1/20 to a factor of 1/10 when the basis of comparison changes from initial true stress to engineering stress. Thus the differences in initial plastic strain between irradiated and unirradiated specimens are significant in evaluating rupture life losses, particularly in the case of high-stress biaxial tests. The use of engineering stress results in a significant apparent difference between uniaxial and biaxial test results. However, the use of initial true stress provides a precise correlation for the data.

Fast reactor irradiation can also affect the creep properties of Type 316 SS as evidenced by the increased creep rates measured in irradiated specimens at 538 °C. Both the minimum creep rate values determined in uniaxial tests and the average creep rate values determined in biaxial tests show the increased creep rate. At a temperature of 538 °C there was very little primary or tertiary creep strain, so the average creep rate in biaxial tests should be a good approximation of the actual minimum creep rate. Minimum creep rates at 593, 649, and 760 °C were apparently not significantly affected by irradiation; however, the average creep rate values indicate that irradiation does not affect creep rates in 649 °C tests, but leads to increased creep rates in 760 °C tests. The

apparent discrepancy between the uniaxial test and the biaxial test in reflecting creep rate changes at 760 °C probably results because the average creep rate is no longer a good approximation of the actual minimum creep rate. Uniaxial tests on the unirradiated tubular material at 760 °C indicated there was substantial primary creep strain; however, this primary creep strain is included as linear creep strain in computing average creep rates from the diametral strains. When primary creep becomes significant, it is quite possible to obtain higher average creep rate values for irradiated specimens, even though the actual minimum creep rate is the same in both irradiated specimens and unirradiated specimens.

Standring et al⁽¹⁾ have reported results on tubes irradiated in DFR and tested in a biaxial stress mode. They observed decreased rupture life for a given effective initial hoop stress, decreased ductility, and no change in average creep rate for tests at 650 °C. The results observed in biaxial tests in the present study at 649 °C are in qualitative agreement with these results. Creep-rupture tests on uniaxial specimens after fast reactor irradiation in DFR have been reported by Weisz et al⁽³⁾. These observations indicated testing at 700 °C after irradiation at 600 °C to a total fluence of 1.6×10^{22} n/cm² resulted in increased minimum creep rates. The results in the present study for uniaxial tests at 649 and 760 °C indicated little if any change in the minimum creep rate. The exact cause of the variance between the two sets of data is not clear, but quite possibly was related to differences in the irradiation temperature, alloy composition, and/or fluence.

A clear picture of the mechanism responsible for the increased creep rates at 538 °C has not yet emerged, but several possible explanations are currently being evaluated. One consideration is that the increased creep rate is a result of

irradiation-induced precipitation that has been observed in the as-irradiated uniaxial material.⁽⁴⁾ A current investigation⁽⁵⁾ of unirradiated, thermally aged specimens of the uniaxial test material does indeed indicate that for aging temperatures above 600 °C extensive precipitation can lead to increased creep rates similar to those observed in irradiated specimens. Although the relationship between the structure and the creep rate in material which has undergone extensive second phase precipitation is not yet established, the present evidence identifies irradiation-induced precipitation as one explanation of the increased creep rates.

Another possible explanation for the creep behavior centers on the irradiation-induced defect structure. Transmission electron microscopy observations showed a low density of voids and dislocations in the as-irradiated uniaxial test material. Increased creep rates could result if this substructure somehow leads to an increased density or increased velocity of mobile dislocations during creep. At higher test temperatures, increased creep rates may not be observed if the substructure annealed out before beginning the creep test. At the present time, there is no direct evidence or detailed theory to support these hypotheses. However, several irradiated specimens have been annealed for 50 hours at 649 °C before creep testing at 538 °C. These specimens still exhibited higher creep rates than unirradiated specimens, so a simple picture of radiation-damage annealing is apparently an inadequate explanation of the observed effects. Also, current studies⁽⁵⁾ of this same alloy continue to show increased creep rates at 538 °C over quite a wide range of irradiation temperatures and fluences. Therefore, if the observed creep behavior is directly related to the irradiation-induced defect structure, the relationship is apparently a complex one.

The magnitude of rupture life loss after irradiation depends on test temperature, and is related to the changes in creep rates and to reduced ductility. At 538 °C, the substantial loss in rupture life was primarily a result of the high creep rates, and the contribution from any ductility loss was relatively small. However, at temperatures of 593, 649, and 760 °C, the losses in rupture life resulted from reduced ductility (i.e., reduced second stage and third stage creep strains), with no significant contribution from creep rate differences. The ductility loss was most severe at 760 °C, and, correspondingly, a larger reduction in rupture life was observed at this temperature. The underlying cause of the low ductility at these higher temperatures was undoubtedly associated with a helium embrittlement mechanism, perhaps operating in conjunction with effects produced by the defect structure and second-phase precipitations.

REFERENCES

1. J. Standring, I. P. Bell, H. Tickel, and A. Glendinning. 'Effects of Neutron Irradiation on Creep-Rupture Properties of Type 316 Stainless Steel Tubes,' "Irradiation Effects in Structural Alloys for Thermal and Fast Reactors," Am. Soc. Testing Mater. Spec. Tech. Publ., vol. 457, pp. 414-428. 1969.
2. W. T. Lee. Biaxial Stress-Rupture Properties of Austenitic Stainless Steels in Static Sodium, A-1-AEC-12694. June 1968.
3. M. Weisz, J. Malkin, J. Erler, and J. P. Andre. 'High Temperature Embrittlement of AISI Type 316 Austenitic Stainless Steels After Irradiation,' "Irradiation Effects in Structural Alloys for Thermal and Fast Reactors," Am. Soc. Testing Mater. Spec. Tech. Publ. vol. 457, pp. 352-370. 1969.
4. H. R. Brager, and H. E. Kissinger. "Irradiation-Induced Precipitation in Type 316 Stainless Steel," Trans, Am. Nucl. Soc., vol. 12, p. 118. 1969.
5. A. J. Lovell, and L. D. Blackburn. Unpublished Data. WADCO Corporation, Richland, Washington. (To be published)

DISTRIBUTION

No. of
Copies

OFFSITE

1 AEC Chicago Patent Group
 G. H. Lee

26 AEC Division of Reactor Development and Technology
 Director, RDT
 Asst Dir for Nuclear Safety
 Analysis & Evaluation Br, RDT:NS
 Asst Dir for Plant Engrg, RDT
 Facilities Br, RDT:PE
 Components Br, RDT:PE
 Instrumentation & Control Br, RDT:PE
 Liquid Metal Systems, Br, RDT:PE
 Asst Dir for Program Analysis, RDT
 Asst Dir for Project Mgmt, RDT
 Liquid Metals Projects Br, RDT:PM
 G. J. Mishko
 FFTF Project Manager, RDT:RE
 Asst Dir for Reactor Engrg, RDT
 Control Mechanisms Br, RDT:RE
 Core Design Br, RDT:RE (2)
 Fuel Handling Br, RDT:RE
 Reactor Vessels, Br, RDT:RE
 Coolant Chemistry Br, RDT:RT
 Fuel Recycle Br, RDT:RT
 Fuels & Materials Br, RDT:RT
 Reactor Physics Br, RDT:RE
 Special Technology Br, RDT:RT
 LMFBR Program Manager, RDT:PM
 Asst Dir for Engrg Standards, RDT
 Fuel Engineering Br, RDT:RE

226 AEC Division of Technical Information Extension

1 AEC Idaho Operation Office
 Nuclear Technology Division
 C. W. Bills, Director

1 AEC San Francisco Operations Office
 Director, Reactor Division

No. of
Copies

5 AEC Site Representatives
 Argonne National Laboratory - CH
 Argonne National Laboratory - ID
 Atomics International
 General Electric Co.
 Westinghouse Electric Corporation

3 Argonne National Laboratory
 R. A. Jaross
 LMFRB Program Office
 N. J. Swanson

1 Atomic Power Development Assoc.
 Document Librarian

5 Atomics International
 FFTF Program Office

2 Babcock & Wilcox Co.
 Atomic Energy Division
 S. H. Esleeck
 G. B. Garton

1 Bechtel Corporation
 J. J. Teachnor

1 Combustion Engineering
 1000 MWe Follow-On Study
 W. P. Staker, Project Manager

1 Combustion Engineering
 911 West Main Street
 Chattanooga, Tennessee 37401
 Mrs. Nell Holder, Librarian

4 General Electric Company
 Advanced Products Operation
 Karl Coben

1 General Electric Company
 Nucleonics Laboratory
 P. O. Box 846
 Pleasanton, California 94566
 Dr. H. W. Alter

No. of
Copies

2 , Gulf General Atomic Inc.
General Atomic Division
D. Coburn

1 Idaho Nuclear Corporation
J. A. Buckham

1 Liquid Metal Engineering Center
R. W. Dickinson

2 Liquid Metal Information Center
A. E. Miller

2 Oak Ridge National Laboratory
W. O. Harms

1 Stanford University
Nuclear Division
Division of Mechanical Engrg
R. Sher

1 United Nuclear Corporation
Research and Engineering Center
R. F. DeAngelis

10 Westinghouse Electric Corporation
Atomic Power Division
Advanced Reactor Systems
D. C. Spencer

ONSITE-HANFORD

1 AEC Chicago Patent Group
R. K. Sharp

2 , AEC Richland Operations Office
J. M. Shivley

3 Battelle Memorial Institute

7 Battelle-Northwest
BNW - Technical Information (5)
BNW - Technical Publication (2)

No. of
Copies

1 Bechtel Corporation
W. A. Smith (Richland)

3 RDT Assistant Director for
Pacific Northwest Laboratories
T. A. Nemzek

100 WADCO Corporation

G. L. Alkire	R. L. Knecht
H. J. Anderson	J. J. Laidler
S. O. Arneson	R. D. Leggett
J. M. Atwood	F. J. Leitz
R. W. Barker (15)	A. J. Lovell (15)
J. M. Batch	D. E. Mahagin
J. F. Bates	W. B. McDonald
R. K. Bierlein	J. S. McMahon
L. D. Blackburn	R. A. Moen
H. R. Bragar	J. M. Norris
C. P. Cabell	M. M. Paxton
J. R. Carrell	R. E. Peterson
T. T. Claudson (2)	B. G. Rieck
J. C. Cochran	W. E. Roake
G. S. Cochrane	G. J. Rogers
W. H. Esselman	W. F. Sheely
E. A. Evans	F. R. Shober
R. L. Fish	J. L. Straalsund
W. M. Gajewski	C. D. Swanson
E. R. Gilbert	J. C. Tobin
G. L. Guthrie	K. G. Toyoda
J. E. Hanson (2)	L. D. Turner
K. M. Harmon	A. L. Ward
E. N. Heck	B. Wolfe
P. L. Hofmann	W. R. Wykoff
J. J. Holmes	WADCO Document Control (15)
J. E. Irvin (2)	WADCO Tech Pubs (703)
J. N. Judy	